Assessing the distribution and growth rates of NO_x emission sources by inverting a 10-year record of NO_2 satellite columns

T. Stavrakou,[1] J.-F. Müller,[1] K. F. Boersma,[2] I. De Smedt,[1] and R. J. van der A[2]

Received 7 February 2008; revised 12 March 2008; accepted 21 April 2008; published 17 May 2008.

[1] Tropospheric NO_2 columns retrieved from the GOME and SCIAMACHY satellite instruments between January 1997 and December 2006 are used together with the IMAGES CTM and its adjoint to construct a top-down inventory for NO_x emissions, with a focus on anthropogenic sources. The influence of the emission updates on the chemical lifetime of NO_x is taken into account, and found to have a significant impact on the results. Anthropogenic emission trends are inferred over industrialized regions of the Northern Hemisphere. The largest emission increases are found over eastern China, and in particular in the Beijing area (growth rate of 9.6%/yr), whereas important emission decreases are calculated over the United States (−4.3%/yr in the Ohio River Valley), and to a lesser extent over Europe (−1.4%/yr in Germany, −1.0%/yr in the Po Basin). The emission changes result in significant trends in surface ozone, amounting to more than 15%/decade over large parts of China in summertime. **Citation:** Stavrakou, T., J.-F. Müller, K. F. Boersma, I. De Smedt, and R. J. van der A (2008), Assessing the distribution and growth rates of NO_x emission sources by inverting a 10-year record of NO_2 satellite columns, *Geophys. Res. Lett.*, *35*, L10801, doi:10.1029/2008GL033521.

1. Introduction

[2] Because of their influence on both tropospheric ozone and the hydroxyl radical (OH), nitrogen oxides (NO_x) are a subject of great interest. The global NO_x emission budget is dominated by fossil fuel combustion, representing more than 60% of the total [*Intergovernmental Panel on Climate Change*, 2001], whereas other more uncertain sources include soils, vegetation fires, and lightning.

[3] Due to rapid economic changes and pollution control legislation, an increasing need arises to provide updated flux estimates, especially in areas where anthropogenic emissions are dominant. Space-based NO_2 columns can help to determine the current source strengths, as well as their evolution during the last decade. Inverse modelling of emissions has been widely used over the last years to derive improved emission estimates of reactive and non-reactive gases using chemistry-transport models (CTMs) and chemical observations, by adjusting the emissions in order to reduce the model/data discrepancies while taking the errors into account. The combination of tropospheric NO_2 data from GOME and SCIAMACHY instruments provides the unprecedented opportunity to investigate the interannual variability and trends in NO_x emissions over the last decade.

[4] Past inversion studies of NO_x emissions include *Jaeglé et al.* [2005], *Martin et al.* [2006], *Konovalov et al.* [2006], and *Wang et al.* [2007]. In addition, trend analysis on the observed columns over China and the eastern U.S. has been performed [*Richter et al.*, 2005; *van der A et al.*, 2006; *Kim et al.*, 2006; *van der A et al.*, 2008]. Note, however, that emission changes are not necessarily proportional to the column changes because of chemical feedbacks involving the hydroxy radical (OH).

[5] In the present study a global top-down inventory of NO_x sources over the last decade is derived, with emphasis on the anthropogenic component of the emissions. The adopted inversion approach relies on the adjoint model technique [*Stavrakou and Müller*, 2006]. The emission fluxes are optimized at the resolution of the model, while automatically accounting for the chemical feedbacks.

2. The Observations and the Inversion Method

[6] We use measurements of tropospheric NO_2 columns retrieved from two UV-visible nadir sounders, GOME between 1997 and 2002, and SCIAMACHY between 2003 and 2006. The data are publicly available at the TEMIS website (www.temis.nl). The individual NO_2 columns and averaging kernels [*Eskes and Boersma*, 2003] are binned onto the horizontal resolution of IMAGES and monthly averaged. The errors include the reported retrieval error [*Boersma et al.*, 2004] and a constant model/representativity error of 10^{15} molec./cm^2. Data are not considered in the inversion when their errors exceed 100%.

[7] An updated version of the IMAGES model [*Müller and Stavrakou*, 2005] is used in this study. It is discretized at $5° \times 5°$ resolution with 40 hybrid sigma-pressure levels in the vertical. The chemical solver is the fourth order Rosenbrock algorithm of the KPP package [*Sandu and Sander*, 2006], with an automatically adjustable timestep. Advection is driven by monthly mean ERA40 reanalysed wind fields till December 2001 and ECMWF operational analyses beyond this date. The daily variability of convective updraught fluxes, PBL mixing, cloud optical depths, temperature and water vapour is accounted for through the ECMWF fields. Horizontal diffusion coefficients are estimated from the ECMWF wind variances. The model time step is equal to one day, and the model calculates daily averaged concentrations. To account for the effect of diurnal variations, the kinetic and photolysis rates are corrected by factors calculated from a full diurnal cycle simulation with a 20-min time step. The NO_2 diurnal

[1] Belgian Institute for Space Aeronomy, Brussels, Belgium.
[2] Royal Netherlands Meteorological Institute, De Bilt, Netherlands.

0094-8276/08/2008GL033521

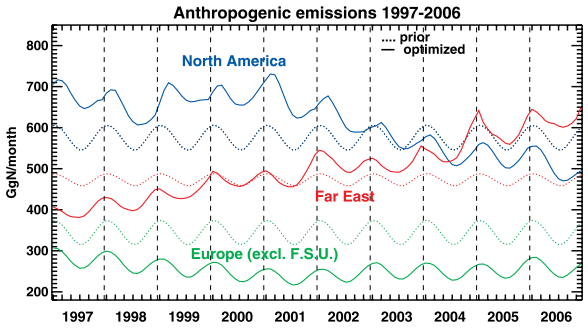

Figure 1. Temporal evolution of anthropogenic NO_x emissions over Europe excluding the F.S.U., N. America (U.S. and Canada), and the Far East (China, Japan, Korea). Dotted and solid lines correspond respectively to the prior and posterior estimates.

profiles calculated from this simulation are also used to estimate the NO_2 concentration at the satellite overpass time from the daily averaged values calculated with a one day time step. The calculation of the monthly NO_2 columns accounts for the averaging kernels and for the sampling times of observations at each location. The chemical mechanism is as in the work by *Müller and Stavrakou* [2005] and the heterogeneous uptake of N_2O_5, NO_3 and HO_2 on the surface of sulphate aerosols is modelled according to *Evans and Jacob* [2005].

[8] Anthropogenic emissions over China are from *Streets et al.* [2003], whereas the EDGARv3.3 inventory for 1997 [*Olivier et al.*, 2001] is used for the rest of the world. Seasonality is taken from *Müller* [1992]. The vegetation fires are distributed according to the GFED version 2 database spanning the period from 1997 to 2006 [*van der Werf et al.*, 2006]. Biogenic NO_x emissions are taken from *Yienger and Levy* [1995] (scaled to 8 Tg N/yr), whereas the NO_x lightning source, scaled globally at 3 Tg N/yr, is distributed according to *Price et al.* [1997] and *Pickering et al.* [1998].

[9] The grid-based inversion approach adopted in this study has been presented in detail by *Stavrakou and Müller* [2006]. The emission fluxes are estimated at the resolution of the model for each emitting process and month between 1997 and 2006 (10x12x72x35 parameters by category). For an emission category, a parameter is optimized in a given grid cell only when the value of the prior maximum emission in the 10-year period in this cell exceeds 10^9 molec.cm^{-2}sec^{-1}. This requirement reduces the number of the emission parameters to be determined: anthropogenic sources (~66,000 parameters), vegetation fires (~70,000), soils (~80,000), and lightning (~90,000). The inversion is performed using the discrete adjoint of the IMAGES model [*Müller and Stavrakou*, 2005]. The relative error on the anthropogenic emissions by a country is taken equal to 0.4 (OECD countries) or 0.7 (for other countries), whereas errors are taken equal to 0.6 for soil and lightning emissions, and to 0.7 for the vegetation fires.

3. Results

[10] Top-down global anthropogenic emissions increase moderately from 1997 to 2002 (by up to 4%), but show a decline (by up to 3%) with respect to the prior after this year. A negative trend of about 5% on the global total is estimated from the inversion between 1997 and 2006. The temporal evolution of this emission source for industrialized regions is illustrated in Figure 1. The NO_x emission over the Far East increases by about 60% over the decade, representing 30% of the global anthropogenic source in 2006, whereas important reductions of North American and European emissions are deduced by the optimization (26 and 9%, resp.). Top-down country emissions in 1997 and the corresponding annual average growth rate are shown in Table 1. The vegetation fire source is found to be slightly reduced on the global scale. Significant decreases are inferred during important fire events, as for instance in Indonesia during fall 1997 and central Africa during the dry season. These decreases might be partly explained by the absence of aerosol correction in the NO_2 columns [*van Noije et al.*, 2006], and/or by a real overestimation in the GFEDv2 inventory.

[11] The inferred increase by 25–55% of the soil NO_x source with respect to the prior source is in agreement with previous studies using also GOME columns [*Jaeglé et al.*, 2005; *Müller and Stavrakou*, 2005]. No evidence, however, is found in our study for enhanced soil emissions over east China, as suggested by *Wang et al.* [2007]. Posterior NO_x emissions from lightning increase by 50–80% with respect to the prior. The updated values are consistent with the estimates by *Boersma et al.* [2005] and *Schumann and Huntrleser* [2007]. Note, however, that the strongest increases of soil and lightning emissions are found in the Tropics, where the BIRA/KNMI columns are systematically higher compared to retrieved columns by other groups [*van Noije et al.*, 2006].

[12] In order to illustrate the inversion results in highly industrialized regions, Figure 2 shows a comparison between the observed monthly averaged NO_2 columns and the modelled prior and posterior columns at the grid cells comprising two megacities, Beijing and Shanghai, China, and two industrial regions, Po Basin, Italy, and Indiana/Ohio River Valley, U.S. The posterior anthropogenic emission strengths inferred at these locations are also illustrated, as well as the annual growth rate (assuming that the emission grows exponentially). The estimated growth rate of anthropogenic emissions of 9.6%/yr in Beijing reflects the rapidly expanding Chinese economy, which over the past twenty years, achieved an average growth rate of nearly 10%/yr [*National Bureau of Statistics of China*, 2006]. It is also very similar to the growth rate of the NO_2 columns over Beijing reported by *van der A et al.* [2008] for 1996–2005. Further, comparison between the growth rate of the

Table 1. Anthropogenic Emissions and Growth Rates by Country[a]

Country	Top-Down Emission in 1997 (Tg N)	Annual Growth Rate 1997–2006 (%/yr)
China	3.33	7.3
USA	6.10	−3.8
Japan	0.93	−1.2
Germany	0.54	−1.3
UK	0.48	−1.7
France	0.33	−1.4

[a]Uncertainties on growth rates are 3.5% for China and 1.8% for the other countries.

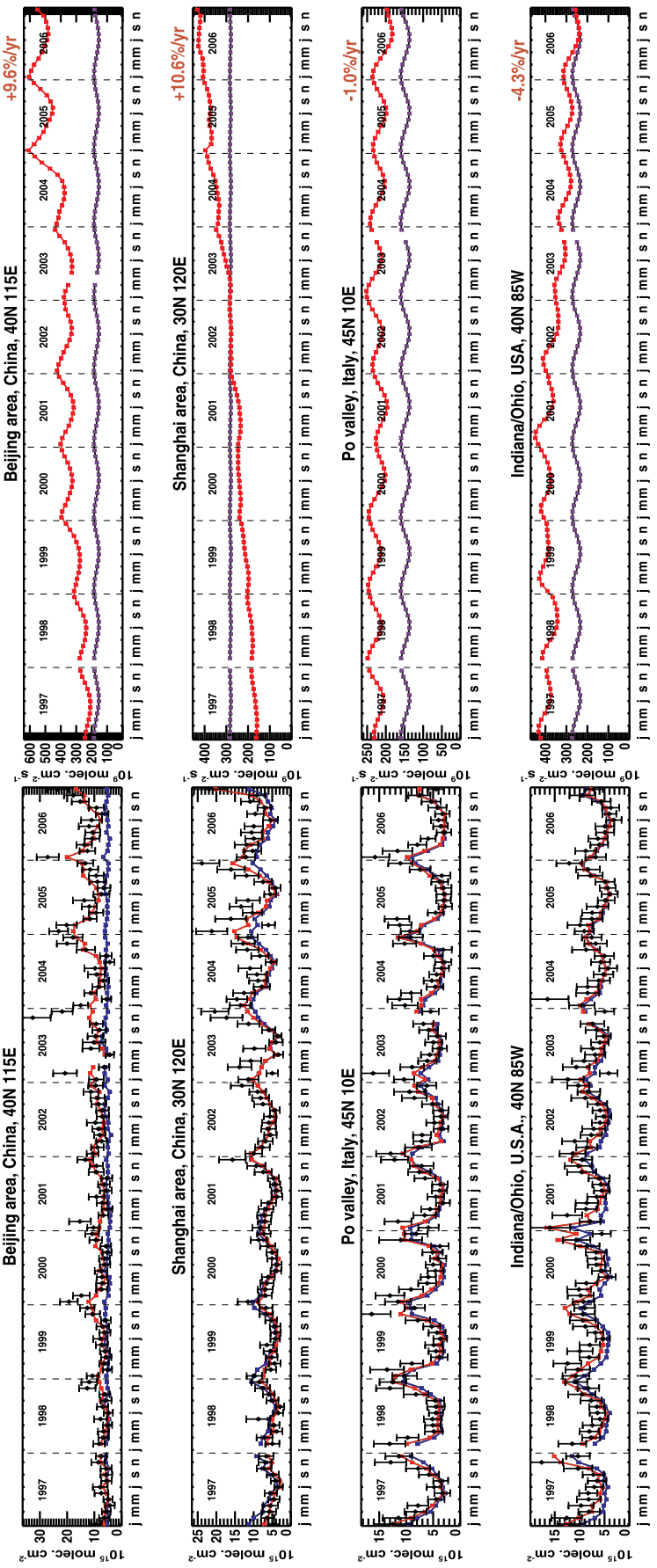

Figure 2. (left) Prior (in blue) and optimized (in red) monthly averaged NO_2 columns compared to the satellite retrievals (diamonds) at four locations. (right) Prior (in blue), updated (in red) anthropogenic NO_x emissions and inferred growth rates.

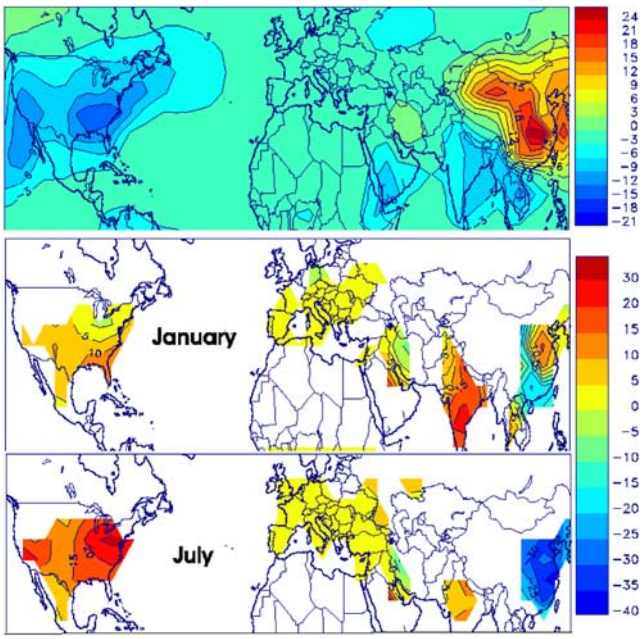

Figure 3. (top) Calculated change (%) in surface O_3 in July due to the anthropogenic NO_x emission change over 1997–2006. (bottom) Calculated change (%) in the lifetime of the NO_2 column due to the anthropogenic NO_x emission changes between 1997 and 2006. The calculation of the NO_2 columns takes into account the averaging kernels of the instrument.

observed columns over China (6.1%/yr) and the corresponding rate reported by *Richter et al.* [2005] (6.7%/yr) over 1997–2002 shows a quite satisfactory agreement between the two retrievals.

[13] Emission abatement strategies targeting coal-fired power plants and other industries are responsible for the anthropogenic emission reductions inferred over the industrial regions of Po Basin and Ohio. The reduction is found to be more important in the Ohio River Valley (annual: −4.3%/yr), especially in summertime (−4.7%/yr), where the inferred posterior NO_x emissions are decreased by 35% between July 1997 and 2006, in agreement with the reductions reported by *Kim et al.* [2006] for summertime. Large growth rates in anthropogenic emissions inferred in other Chinese cities, like Shanghai (10.6%/yr), Jinan (9.1%/yr) and Harbin (8.8%/yr), are generally in good agreement with the corresponding values in the observed columns [*van der A et al.*, 2006, 2008]. The annual rate of 6%/yr in the updated emissions over Tehran, Iran is also in accordance with the 1999 economic growth rate of 4.1% reflecting the growing trend of electricity consumption, newly constructed power plants, and increased vehicle use [*Rostamihozori*, 2002]. In Central Germany, the inferred decrease by 11% of the 2006 emissions with respect to the 1997 values (−1.4%/yr) is a result of the emission controls and the efficient use of new technologies (catalytic converters).

[14] The calculated change in surface ozone mixing ratio in July due to the change in anthropogenic NO_x emissions over 1997–2006 is displayed in the top plot of Figure 3. The highest increase is inferred west of Shanghai (>20%), whereas increases of more than 15% are found over large parts of China. The ozone increase in Beijing region is more moderate (11%) and is found to be in qualitative agreement with the significant ozone trend (2%/yr) deduced by *Ding et al.* [2008] over Beijing based on one decade of MOZAIC airborne data. No significant trend, however, is calculated for CO concentrations over 1997–2006 due to the change in NO_x source strengths, in consistency with GAW ground-based CO measurements (gaw.kishou.go.jp/wdcgg.html) downwind of China. Further, in response to the power plant emission controls, the inversion infers ozone decreases by 9% over the Indiana/Ohio region, in quite good agreement with *Kim et al.* [2006].

[15] Chemical feedbacks of the NO_x-OH system play a significant role in the inversion, as illustrated in the two bottom plots of Figure 3 showing the calculated change in lifetime of the NO_2 column due to the anthropogenic NO_x emission change between 1997 and 2006. Over the Far East, the NO_x emission increase results in enhanced OH production in summertime (due to the NO + HO_2 reaction), which leads to an increase of the NO_2 loss through OH, and therefore to a decrease of the NO_x lifetime (>25%), which explains the moderate increase of the observed summertime NO_2 columns. Over the US, the NO_x emission reductions imply an increase of the NO_x lifetime, which is more significant over the North Eastern US (>15%). During winter, the NO_x emission increases lead to a decrease of OH (NO_2 + OH sink), and consequently, to longer NO_x lifetimes (by about 10% over Northern China), and to higher NO_2 columns, as shown in Figure 2 for Beijing and Shanghai regions.

[16] Quantitatively, while the growth rate of the observed columns in Beijing region is only 5.3%/yr in summertime, it reaches 11.8%/yr in wintertime, although the inferred emission rate is ∼9% in both seasons (Figure 2). This example highlights the non-linear relationship between NO_x emissions and NO_2 columns, contradicting the assumption of a linear dependency [e.g., *Richter et al.*, 2005].

4. Conclusions

[17] The distribution and trends of NO_x emissions have been determined from tropospheric NO_2 columns retrieved by the GOME/SCIAMACHY satellite instruments, based on the IMAGES CTM, providing the relationship of NO_2 columns to NO_x emissions, and the adjoint-based methodology. Optimizing at the spatial resolution of the model allows to improve for the fine scale distribution, the seasonality and the interannual variability of the emissions. Updated emission strengths enable important reduction of the model/data discrepancies, and emission growth rates are inferred for anthropogenic emissions thanks to the long-term observation record used.

[18] The soil and lightning NO_x emissions deduced by the inversion are found to be underestimated in the prior inventory, in agreement with previous studies. Whereas emission abatement strategies and a moderate economical growth result in significant emission decreases over Europe (9%), Japan (25%) and the U.S. (26%), the emissions over Far East have increased by 60% over the last decade, at an average rate of 5.1%/yr. The strongest annual anthropogenic

emission growth rates are inferred over Beijing and Shanghai areas (~10%), while the highest decline rates are found over the Ohio industrial area (−4.3%/yr). In China, chemical feedbacks explain the NO_2 column enhancement in wintertime compared to summertime, and the resulting increased seasonality in the observed columns. In response to the emission changes, surface ozone is calculated to increase by more than 15% over large parts of China in summertime.

[19] **Acknowledgments.** This work has been supported by the PRODEX programme of the ESA funded by the Belgian Science Policy.

References

Boersma, K. F., H. J. Eskes, and E. J. Brinksma (2004), Error analysis for tropospheric NO_2 retrieval from space, *J. Geophys. Res.*, *109*, D04311, doi:10.1029/2003JD003962.

Boersma, K. F., H. J. Eskes, E. W. Meijer, and H. M. Kelder (2005), Estimates of lightning NO_x production from GOME satellite observations, *Atmos. Chem. Phys.*, *5*, 2311–2331.

Ding, A. J., T. Wang, V. Thouret, J.-P. Cammas, and P. Nédélec (2008), Tropospheric ozone climatology over Beijing: Analysis of aircraft data from the MOZAIC program, *Atmos. Chem. Phys*, *8*, 1–13.

Eskes, H. J., and K. F. Boersma (2003), Averaging kernels for DOAS total-column satellite retrievals, *Atmos. Chem. Phys*, *3*, 1285–1291.

Evans, M. J., and D. J. Jacob (2005), Impact of new laboratory studies of N_2O_5 hydrolysis on global model budgets of tropospheric nitrogen oxides, ozone, and OH, *Geophys. Res. Lett.*, *32*, L09813, doi:10.1029/2005GL022469.

Jaeglé, L., L. Steinberger, R. V. Martin, and K. Chance (2005), Global partitioning of NOx sources using satellite observations: Relative roles of fossil fuel combustion, biomass burning and soil emissions, *Faraday Discuss.*, *130*, 407–423, doi:10.1039/b502128f.

Intergovernmental Panel on Climate Change (2001), *Climate Change 2001: The Scientific Basis. Contribution of Working Group I to the Third Assessment Report of the Intergovernmental Panel on Climate Change*, edited by J. T. Houghton et al., Cambridge Univ. Press, Cambridge, U. K.

Kim, S.-W., A. Heckel, S. A. McKeen, G. J. Frost, E.-Y. Hsie, M. K. Trainer, A. Richter, J. P. Burrows, S. E. Peckham, and G. A. Grell (2006), Satellite-observed U.S. power plant NO_x emission reductions and their impact on air quality, *Geophys. Res. Lett.*, *33*, L22812, doi:10.1029/2006GL027749.

Konovalov, I. B., M. Beekmann, A. Richter, and J. P. Burrows (2006), Inverse modelling of the spatial distribution of NO_x emission on the continental scale using satellite data, *Atmos. Chem. Phys.*, *6*, 1747–1770.

Martin, R. V., C. E. Sioris, K. Chance, T. B. Ryerson, T. H. Bertram, P. J. Wooldridge, R. C. Cohen, J. A. Neuman, A. Swanson, and F. M. Flocke (2006), Evaluation of space-based constraints on global nitrogen oxide emissions with regional aircraft measurements over and downwind of eastern North America, *J. Geophys. Res.*, *111*, D15308, doi:10.1029/2005JD006680.

Müller, J.-F. (1992), Geographical distribution and seasonal variation of surface emissions and deposition velocities of atmospheric trace gases, *J. Geophys. Res.*, *97*, 3787–3804.

Müller, J.-F., and T. Stavrakou (2005), Inversion of CO and NO_x emissions using the adjoint of the IMAGES model, *Atmos. Chem. Phys.*, *5*, 1157–1186.

National Bureau of Statistics of China (2006), *China Statistical Yearbook*, 25th ed., China Stat., Beijing.

Olivier, J. G. J., et al. (2001), Applications of EDGAR. Including a description of EDGAR 3.0: Reference database with trend data for 1970–1995, *RIVM Rep. 773301 001*, Natl. Inst. for Public Health and Environ., Bilthoven, Netherlands.

Pickering, K. E., Y. Wang, W. K. Tao, C. Price, and J.-F. Müller (1998), Vertical distributions of lightning NO_x for use in regional and global chemical transport models, *J. Geophys. Res.*, *103*, 31,203–31,216.

Price, C., J. Penner, and M. Prather (1997), NO_x from lightning: 1. Global distribution based on lightning physics, *J. Geophys. Res.*, *102*, 5929–5941.

Richter, A., J. P. Burrows, H. Nüß, C. Granier, and U. Niemeier (2005), Increase in tropospheric nitrogen oxide over China observed from space, *Nature*, *437*, 129–132.

Rostamihozori, N. (2002), Development of energy and emission control strategies for Iran, Ph.D. dissertation, Univ. of Karlsruhe, Karlsruhe, Germany.

Sandu, A., and R. Sander (2006), Technical note: Simulating chemical systems in Fortran90 and Matlab with the Kinetic PreProcessor KPP-2.1, *Atmos. Chem. Phys.*, *6*, 187–195.

Schumann, U., and H. Huntrleser (2007), The global lightning-induced nitrogen oxides source, *Atmos. Chem. Phys.*, *7*, 2623–2816.

Stavrakou, T., and J.-F. Müller (2006), Grid-based versus big region approach for inverting CO emissions using Measurement of Pollution in the Troposphere (MOPITT) data, *J. Geophys. Res.*, *111*, D15304, doi:10.1029/2005JD006896.

Streets, D. G., et al. (2003), An inventory of gaseous and primary aerosol emissions in Asia in the year 2000, *J. Geophys. Res.*, *108*(D21), 8809, doi:10.1029/2002JD003093.

van der A, R. J., D. H. M. U. Peters, H. Eskes, K. F. Boersma, M. Van Roozendael, I. De Smedt, and H. M. Kelder (2006), Detection of the trend and seasonal variation in tropospheric NO_2 over China, *J. Geophys. Res.*, *111*, D12317, doi:10.1029/2005JD006594.

van der A, R. J., H. J. Eskes, K. F. Boersma, T. P. C. van Noije, M. Van Roozendael, I. De Smedt, D. H. M. U. Peters, and E. W. Meijer (2008), Trends, seasonal variability and dominant NOx source derived from a ten year record of NO_2 measured from space, *J. Geophys. Res.*, *113*, D04302, doi:10.1029/2007JD009021.

van der Werf, G. R., et al. (2006), Interannual variability in global biomass burning emissions from 1997 to 2004, *Atmos. Chem. Phys.*, *6*, 3423–3441.

van Noije, T. P. C., et al. (2006), Multi-model ensemble simulations of tropospheric NO_2 compared with GOME retrievals for the year 2000, *Atmos. Chem. Phys.*, *6*, 2943–2979.

Wang, Y., M. B. McElroy, R. V. Martin, D. G. Streets, Q. Zhang, and T.-M. Fu (2007), Seasonal variability of NO_x emissions over east China constrained by satellite observations: Implications for combustion and microbial sources, *J. Geophys. Res.*, *112*, D06301, doi:10.1029/2006JD007538.

Yienger, J. J., and H. Levy (1995), Empirical model of global soil-biogenic NO_x emissions, *J. Geophys. Res.*, *100*, 11,447–11,464.

K. F. Boersma and R. J. van der A, Royal Netherlands Meteorological Institute, NL-3730 AE De Bilt, Netherlands.

I. De Smedt, J.-F. Müller, and T. Stavrakou, Belgian Institute for Space Aeronomy, Avenue Circulaire 3, B-1180, Brussels, Belgium. (jenny@aeronomie.be)